Magnetic Polarons in the 1D FM Kondo Model

Winfried Koller, Alexander Prüll, Hans Gerd Evertz, and Wolfgang von der Linden

Institut für Theoretische Physik, Technische Universität Graz, Petersgasse 16, A-8010 Graz, Austria.[*]

(Dated: January 20, 2003)

The ferromagnetic Kondo model with classical corespins is studied via unbiased Monte-Carlo simulations. We show that with realistic parameters for the manganites and at low temperatures, the double-exchange mechanism does not lead to phase separation in one-dimensional chains but rather stabilizes individual ferromagnetic polarons. Within the ferromagnetic polaron picture, the pseudogap in the one-particle spectral function $A_k(\omega)$ can easily be explained. Ferromagnetic polarons also clear up a seeming failure of the double-exchange mechanism in explaining the comparable bandwidths in the ferromagnetic and paramagnetic phase. For our analysis, we extend a simplified model, the finite temperature uniform hopping approach (UHA), to include polarons. It can easily be evaluated numerically and provides a simple quantitative understanding of the physical features of the ferromagnetic Kondo model.

I. INTRODUCTION

Manganese oxides such as $La_{1-x}Sr_xMnO_3$ and $La_{1-x}Ca_xMnO_3$ have been attracting considerable attention since the discovery of colossal magnetoresistance (CMR)[1,2]. These materials crystalize in the perovskite-type lattice structure where the crystal field breaks the symmetry of the atomic wave function of the manganese d-electrons. The energetically lower t_{2g} levels are occupied by three localized electrons. Due to a strong Hund coupling their spins are aligned, forming a localized corespin with $S = 3/2$. The electron configuration of the Mn^{3+} ions is $t_{2g}^3 e_g^1$, whereas for Mn^{4+} ions the e_g electron is missing. Due to a hybridization of the e_g wave function with the oxygen $2p$ orbitals, the e_g electrons are itinerant and can move from an Mn^{3+} ion to a neighboring Mn^{4+} via a bridging O^{2-}. The interplay of various physical ingredients such as the strong Hund coupling (J_H) of the itinerant electrons to localized corespins, Coulomb correlations, and electron-phonon coupling leads to a rich phase diagram including antiferromagnetic insulating, ferromagnetic metallic and charge ordered domains. The dynamics of the charge carriers moving in the spin and orbital background shows remarkable dynamical features[3,4].

Since full many-body calculations for a realistic model, including all degrees of freedom, are not possible yet, several approximate studies of simplified models have been performed in order to unravel individual pieces of the rich phase diagram of the manganites. The electronic degrees of freedom are generally treated by a Kondo lattice model which in the strong Hund coupling limit is commonly referred to as the double-exchange (DE) model, a term introduced by Zener[5]. In addition, the correlation of the itinerant e_g electrons is well described by a nearest neighbor (n.n.) Coulomb interaction. The on-site Hubbard term merely renormalizes the already strong Hund coupling. For the Kondo model with quantum spins it is still impossible to derive rigorous numerical or analytical results. If the S=3/2 corespins are treated classically, however, the model can be treated by unbiased Monte Carlo techniques. The impact of quantum spins on the electronic properties has been studied in Ref. 6,7,8. It appears that quantum effects are important for (S=1/2) corespins or at $T = 0$. For finite temperature and S=3/2, classical spins present a reasonable approximation.

Elaborate Monte Carlo (MC) simulations for the FM Kondo model with classical t_{2g} corespins have been performed by Dagotto *et al.*[9,10,11], Yi *et al.*[12], and by Furukawa *et al.*[13,14]. Static and dynamical properties of the model have been determined. These studies revealed features (discontinuity of the mean electron density as a function of the chemical potential, infinite compressibility) which have been interpreted as signatures of phase-separation (PS). PS has also been reported[15] from computations based on a dynamical mean field treatment of the DE model at $T = 0$. A phase diagram and critical exponents of the DE model have been determined with a Hybrid MC algorithm[16,17].

In the manganites, the Hund coupling J_H is much stronger than the kinetic energy. Consequently, configurations are very unlikely in which the electronic spin is antiparallel to the local corespin. The present authors have proposed an effective spinless fermion (ESF) model[18] that takes effects of antiparallel spin configurations into account via virtual excitations. It has been demonstrated that the results of the ESF model are in excellent agreement with those of the original Kondo model even for moderate values of J_H. This applies also to features which have been previously interpreted as signatures of PS[11]. Taking Coulomb interactions into account, PS has been argued to lead to either small[19] or large[20] (nano-scale) clusters, which have been the basis for a possible though controversial[6] explanation of CMR[21,22]. Moreover, lattice distortions[23,24] are believed to play a crucial role for the CMR effect[6,25] and should also be included in the model.

In this paper, we present a numerical and analytical study of the 1D ferromagnetic Kondo model with classical corespins. We find that the correct physical inter-

pretation of the features which have been interpreted as PS in the one-dimensional model, is rather given by ferromagnetic polarons, i.e. small FM-regions with *one single* trapped charge-carrier, compatible with exact diagonalization results for small clusters[3]. This applies even without n.n. Coulomb repulsion invoked in Refs 19,20. Energetically, there is no significant difference between polarons, bi-polarons or even charge accumulations in the PS sense. It is rather the entropy, which even near zero temperature clearly favors polarons. The polaron picture allows also a straight forward and obvious explanation of the pseudogap, which has been previously observed in the spectral density[18,21,26,27].

In a previous paper[18] we introduced the uniform hopping approximation (UHA), which replaces the influence of the random corespins on the e_g electron dynamics by an effective uniform hopping process. Essential physical features of the original model could be described even quantitatively by UHA, while the configuration space, and hence the numerical effort, was reduced by several orders of magnitude. Besides the numerical advantage, UHA also allows the derivation of analytical results in some limiting cases at $T = 0$.

In Ref. 28 we have extended UHA to finite temperatures by allowing for thermal fluctuations of the uniform hopping parameter. By taking into account the density of corespin states, it is possible to calculate thermodynamic quantities of one and three-dimensional systems in the UHA. The reliability of this finite-temperature UHA has been scrutinized by a detailed comparison of the results for various properties of the ferromagnetic Kondo model with unbiased MC data in 1D.

Here, we will generalize UHA to regimes, where a single hopping parameter is not sufficient to describe the physics of the FM Kondo model. Particularly near half filling, a typical corespin configuration shows small ferromagnetic domains (polarons) immersed in an antiferromagnetic background. Therefore, two different UHA-parameters are necessary to model the impact of the fluctuating corespins on the e_g electron dynamics.

This paper is organized as follows. In Sec. II the model Hamiltonian is presented and particularities of the MC simulation for the present model are outlined. The general discussion of ferromagnetic polarons near half filling is presented in Sec. III. Section IV develops a generalization of the uniform hopping approach in order to treat FM polarons. Polaronic features in the spectral density are analyzed. The key results of the paper are summarized in Sec. V.

II. MODEL HAMILTONIAN AND UNBIASED MONTE CARLO

In this paper, we will concentrate solely on properties of the itinerant e_g electrons interacting with the *local* t_{2g} corespins. We also neglect the degeneracy of the e_g orbitals. The degrees of freedom of the e_g electrons are

then described by a single-orbital Kondo lattice model[28]. As proposed by de Gennes[29], Dagotto *et al.*[9,21] and Furukawa[13], the t_{2g} spins $\mathbf{S}_i$ are treated classically, which is equivalent to the limit $S \to \infty$. The spin degrees of freedom ($\mathcal{S}$) are thus replaced by unit vectors $\mathbf{S}_i$, parameterized by polar and azimuthal angles θ_i and ϕ_i, respectively. The magnitude of both corespins and e_g-spins is absorbed into the exchange couplings.

A. Effective Spinless Fermions

It is expedient to use the individual t_{2g} spin direction $\mathbf{S}_i$ as the local quantization axis for the spin of the itinerant e_g electrons at the respective sites. This representation is particularly useful for the $J_H \to \infty$ limit, but also for the projection technique, which takes into account virtual processes for finite Hund coupling. As described in Ref. 18, the energetically unfavorable states with e_g electrons antiparallel to the local t_{2g} corespins can be integrated out. This yields the 1D effective spinless fermion model (ESF)

$$\hat{H} = - \sum_{<i,j>} t_{i,j}^{\uparrow\uparrow} c_i^\dagger c_j - \sum_{i,j} \frac{t_{i,j}^{\uparrow\downarrow} t_{j,i}^{\downarrow\uparrow}}{2J_H} c_i^\dagger c_i + J' \sum_{<i,j>} \mathbf{S}_i \cdot \mathbf{S}_j \, . \tag{1}$$

The spinless fermion operators c_j correspond to spin-up electrons (relative to the *local* corespin-orientation) only. The spin index has, therefore, been omitted. With respect to a *global* spin-quantization axis the ESF model (1) still contains contributions from both spin-up and spin-down electrons.

The first term in Eq. (1) corresponds to the kinetic energy in tight-binding approximation. The modified hopping integrals $t_{i,j}^{\sigma,\sigma'}$ depend upon the t_{2g} corespin orientation

$$t_{i,j}^{\sigma,\sigma'} = t_0 \, u_{i,j}^{\sigma,\sigma'} \, , \tag{2}$$

where the relative orientation of the t_{2g} corespins at site i and j enters via

$$\begin{aligned} u_{i,j}^{\sigma,\sigma}(\mathcal{S}) &= \cos(\vartheta_{ij}/2) \, e^{i\psi_{ij}} \\ u_{i,j}^{\sigma,-\sigma}(\mathcal{S}) &= \sin(\vartheta_{ij}/2) \, e^{i\chi_{ij}} \end{aligned} \, . \tag{3}$$

These factors depend on the relative angle ϑ_{ij} of corespins $\mathbf{S}_i$ and $\mathbf{S}_j$ and on some complex phases ψ_{ij} and χ_{ij}.

The second term in Eq. (1) accounts for virtual hopping processes to antiparallel spin–corespin configurations and vanishes in the limit $J_H \to \infty$. The last term is a small antiferromagnetic exchange of the corespins.

It should be noted that the unitary transformation to the local spin quantization axis is not unique. This fact can be exploited to eliminate the phase factors ψ_{ij} in 1D. Then the n.n. hopping integrals are simply given by the real numbers $\cos(\vartheta_{ij}/2)$.

B. Grand Canonical Treatment

We define the grand canonical partition function as

$$\mathcal{Z} = \int \mathcal{D}[\mathcal{S}] \;\; \mathrm{tr}_c \, e^{-\beta(\hat{H}(\mathcal{S}) - \mu\hat{N})}$$

$$\int \mathcal{D}[\mathcal{S}] \; = \prod_{i=1}^{L} \left(\int_0^{\pi} d\theta_i \sin\theta_i \int_0^{2\pi} d\phi_i \right), \quad (4)$$

where tr_c indicates the trace over fermionic degrees of freedom at inverse temperature β, $\hat{N}$ is the operator for the total number of e_g electrons and μ stands for the chemical potential. Upon integrating out the fermionic degrees of freedom, we obtain the statistical weight of a corespin configuration $\mathcal{S}$ that can be written as

$$w(\mathcal{S}) = \frac{\mathrm{tr}_c \, e^{-\beta(\hat{H}(\mathcal{S}) - \mu\hat{N})}}{\mathcal{Z}} \; . \quad (5)$$

Equation (4) is the starting point of Monte Carlo simulations of the Kondo model[9] where the sum over the classical spins is performed via importance sampling. The spin configurations $\mathcal{S}$ enter the Markov chain according to the weight factor $w(\mathcal{S})$ that is computed via exact diagonalization of the corresponding one-particle Hamiltonian in Eq. (1). In the 1D case we have performed MC simulations in which spins in domains of random lengths were rotated. We have performed MC runs with 2000 measurements. The skip between subsequent measurements was chosen to be some hundreds of lattice sweeps reducing autocorrelations to a negligible level.

As previously shown[28], the spin-integrated one-particle Green's function can be written as

$$\sum_{\sigma} \ll a_{i\sigma}; a_{j\sigma}^{\dagger} \gg_{\omega} = \int \mathcal{D}[\mathcal{S}] \; w(\mathcal{S}) u_{ji}^{\uparrow\uparrow}(\mathcal{S}) \ll c_i; c_j^{\dagger} \gg_{\omega}^{\mathcal{S}} , \quad (6)$$

where $\ll c_i; c_j^{\dagger} \gg_{\omega}^{\mathcal{S}}$ is the Green's function in local spin quantization. It can be expressed in terms of the one-particle eigenvalues $\epsilon^{(\lambda)}$ and the corresponding eigenvectors $|\psi^{(\lambda)}\rangle$ of the Hamiltonian $\hat{H}(\mathcal{S})$:

$$\ll c_i; c_j^{\dagger} \gg_{\omega}^{\mathcal{S}} = \sum_{\lambda} \frac{\psi^{(\lambda)}(i) \, \psi^{*(\lambda)}(j)}{\omega - (\epsilon^{(\lambda)} - \mu) + i0^+}$$

It should be pointed out that the one-particle density of states (DOS) is independent of the choice of the spin-quantization.

C. Uniform Hopping Approach

The integral over the corespin states in the partition function (4) can be evaluated approximatively by resorting to a uniform hopping approach (UHA)[28]. The key idea is to replace the impact of the locally fluctuating corespins on the hopping amplitudes by some global average quantity u. Then the Hamiltonian merely depends
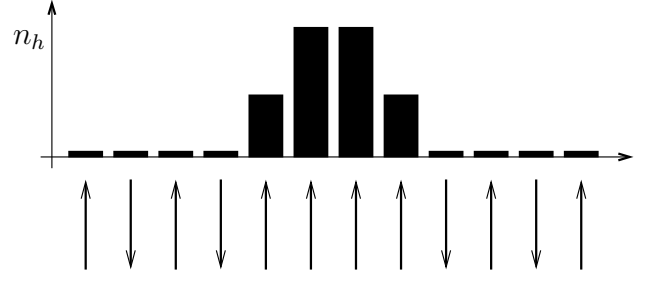

FIG. 1: Idealized spin and hole-density configuration in a 1D Kondo chain at the critical chemical potential μ^*. A FM domain of $L_f = 4$ lattice sites is embedded in an AFM background. A single hole is localized in the FM domain giving rise to the depicted hole density (different from the schematic shape in Fig 4 of Ref. 30).

on one parameter, namely u, and the partition function can be written as the one-dimensional integral

$$\mathcal{Z} = \int_0^1 du \, \Gamma(u) \; \mathrm{tr}_c \, e^{-\beta(\hat{H}(u) - \mu\hat{N})} \; .$$

The density of corespin states $\Gamma(u)$ can be obtained numerically for 3D systems and analytically for 1D systems.

Obviously, this simplification assumes a uniform medium. In order to cope with magnetic polarons, the UHA has to be generalized and $\Gamma(u)$ should be replaced by a two-parameter density $\Gamma(u_f, u_a)$, where $u_f(u_a)$ denotes the average hopping within the (anti)ferromagnetic domains. The details and results of such a generalization are the contents of Sec. IV of this paper.

III. FERROMAGNETIC POLARONS

Near half filling of a single e_g band, a tendency towards phase separation has been observed in various studies. It has been claimed that the system separates into FM domains of high carrier concentration and AFM domains of low carrier concentration. In the following we show that a different picture rationalizes the 1D Monte Carlo results in the range $n \approx 0.7 - 1.0$.

We show that ferromagnetic polarons, i.e. *single* charge carriers surrounded by small ferromagnetic spin-clouds, are formed when holes are doped into the half filled e_g band. In order to model such a polaron in a one-dimensional system, we take L_f adjacent lattices sites to be in ferromagnetic order and use $\Gamma_{L-L_f}(u)$ to account for the degeneracy of the remaining spins.

First, we estimate the size L_f of the FM polaron[31] using a simple polaron picture. In this view the hole is confined in a perfectly FM domain consisting of L_f lattice sites and outside the domain the system is in perfect AFM order (see Fig. 1). The tight-binding energies in a potential well (FM domain) with infinite barrier height are

$$\epsilon_\nu = -2 \cos\left(\frac{\nu\,\pi}{L_f+1}\right), \qquad \nu = 1, \ldots, L_f \, . \quad (7)$$

The energy difference between a) a one-polaron state with perfect FM spins within the polaron and perfect AFM order outside and b) perfectly antiferromagnetically ordered t_{2g} spins is given by

$$\Delta\epsilon_p = -2\cos\left(\frac{\pi}{L_f+1}\right) + 2J_{\text{eff}}\left(L_f - 1\right),$$

where the first term accounts for the kinetic (delocalization) energy of the hole in the potential well and the second term describes the energy deficiency due to $(L_f - 1)$ ferromagnetic bonds. We have introduced the effective antiferromagnetic coupling J_{eff}, given by

$$J_{\text{eff}} = J' + 1/(2J_H)$$

near $n \approx 1$ (see Ref. 18). For typical values $J_H = 6$ and $J' = 0.02$ we have $J_{\text{eff}} \approx 0.1$. Upon minimizing $\Delta\epsilon_p$ with respect to L_f, we obtain the optimal size of the polaron, which in the present case lies between $L_f = 3$ and $L_f = 4$. If the FM domain contains $N > 1$ charge carriers, the energy difference is simply

$$\Delta\epsilon_p(N) = -2\sum_{\nu=1}^{N}\cos\left(\frac{\nu\,\pi}{L_f+1}\right) + 2J_{\text{eff}}\left(L_f - 1\right).$$

For $N = 2$, the optimum bi-polaron size is $L_f \simeq 7$ and it increases to $L_f \simeq 10$ for $N = 3$ charge carriers.

Next we estimate the chemical potential μ^*, at which holes start to populate the polaron states. Apart from the energy of the antiferromagnetic t_{2g} spins, the total energy (at $T = 0$) of the filled e_g band is given in the grand canonical ensemble by $-\mu^* L$. By equating this energy to the total energy of the polaron we have

$$-\mu^* L = -\mu^*\left(L - 1\right) + \Delta\epsilon_p(1)$$

which yields the desired chemical potential

$$\mu^* = -\Delta\epsilon_p(1) = 2\cos\left(\frac{\pi}{L_f+1}\right) - 2J_{\text{eff}}\left(L_f - 1\right).$$

The critical chemical potential is depicted in Fig. 2. Similar considerations yield that μ^* also approximately presents the limiting chemical potential between the filled antiferromagnetic band and a state with several single FM polarons, provided the polaron density is low, i.e. as long as we have an antiferromagnetic background. Consequently, at the chemical potential μ^* the electron density is not fixed. The energy gain $\Delta\epsilon_p$ exactly balances the loss of the chemical potenital $-\mu^*$. This implies that the electron density has a discontinuity at μ^*, i.e. the compressibility of the electrons diverges which has been previously interpreted as a consequence of PS tendencies (see Fig. 3a in Ref. 20 and Ref. 13).

If we repeat the considerations for bi-polarons with the respective optimized size ($L_f \simeq 7$ for the standard parameter set), we find a critical chemical potential, also depicted in Fig. 2, which is very close to that of polarons. If we proceed to tri-polarons we find again a
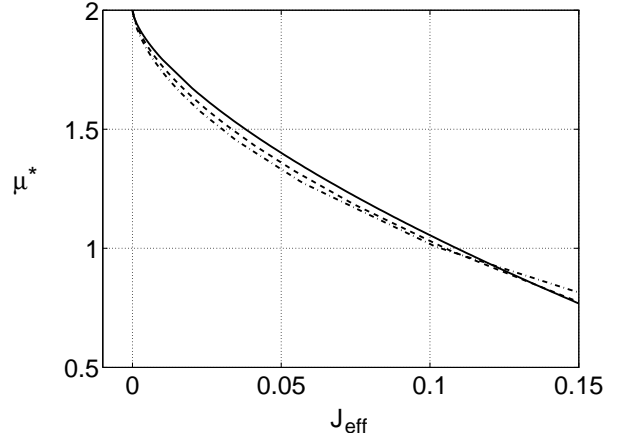

FIG. 2: Critical chemical potential $|\mu^c|$ of the homogeneous model (solid line) from Ref. 18 as compared to the chemical potential μ^* at which polarons (dash dotted) and bipolarons (dashed) start to enter the Kondo chain.

similar μ^*. As can be seen in Fig. 2, the chemical potential μ^* virtually coincides with the chemical potential μ^c of the "phase separation" obtained in Ref. 18. This potential was calculated as the point of coexistence of FM and AFM order in a homogeneous system. In view of the rather rough estimate of μ^* we conclude that polarons, bi-polarons, up to phase separated FM regions, are energetically comparable as long as the size of the FM domains is optimally adapted. For $J_{\text{eff}} \gtrsim 0.12$ which is comparable with the antiferromagnetic exchange in manganites, individual polarons are energetically favored.

FM polarons, however, have a much higher entropy than the other objects and are therefore thermodynamically favored, even at low temperature. Moreover, at $T \neq 0$ the domains are not completely (anti)ferromagnetically aligned which further reduces the energy differences between polaron and bi-polaron/phase-separated states considerably. Therefore, even for values of $J_{\text{eff}} < 0.12$ we find individual polarons at very low temperatures. This conclusion is corroborated at $\beta = 50$ and $J_{\text{eff}} \simeq 0.10$ by the ensuing analysis of MC simulations.

In order to scrutinize the polaron arguments, we compute the mean particle numbers for the corespin configurations entering the Markov chain of unbiased MC

$$\langle\hat{N}\rangle_{\mathcal{S}} := \frac{\text{tr}_c\left(\hat{N}\,e^{-\beta(\hat{H}(\mathcal{S})-\mu\hat{N})}\right)}{\text{tr}_c\left(e^{-\beta(\hat{H}(\mathcal{S})-\mu\hat{N})}\right)} = \sum_{\nu=1}^{L}\frac{1}{1 + e^{\beta(\epsilon_\nu(\mathcal{S})-\mu)}},$$

where $\epsilon_\nu(\mathcal{S})$ are the eigenvalues of $\hat{H}(\mathcal{S})$ for the configuration $\mathcal{S}$. As a consequence of the above reasoning we expect a broad distribution of integer-valued particle numbers if the chemical potential is close to μ^*. The MC time series for $\langle\hat{N}\rangle_{\mathcal{S}}$ for a $L = 50$ site chain ($J_H = 6, J' = 0.02, \beta = 50$) is shown in Fig. 3. One time step corresponds to 1000 sweeps of the lattice. The inverse temperature $\beta = 50$ corresponds to $T \simeq 50-100\,\text{K}$, i.e. a temperature relevant for experiments.
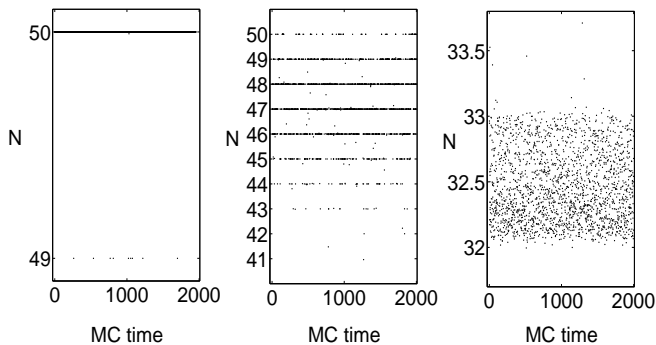
FIG. 3: Mean particle numbers in a grand canonical MC simulation ($L = 50$, $J_H = 6$, $J' = 0.02$, $\beta = 50$) as a function of MC time. One time step corresponds to 1000 sweeps of the lattice. a) AFM case ($\mu = 1.22$) b) polaron regime ($\mu \simeq \mu^* \simeq 1.02$) c) FM regime ($\mu = 0.80$).

The left-hand panel corresponds to a situation where the chemical potential is far above the critical chemical potential, which has the value $\mu^* \simeq 1.02$ for the present parameter set. We see that the band is almost completely filled, with isolated dots at $N_e = 49$ corresponding to occasional FM polarons. At μ^* (central panel), in agreement with the polaron picture we find a broad distribution of *integer-valued* mean particle numbers. If the chemical potential is reduced below μ^*, the system becomes ferromagnetic and we find the standard result of free electrons with a narrow and continuous spread in $\langle \hat{N} \rangle$ not restricted to integer values.

Hole-dressed spin-spin correlations provide another piece of evidence in favor of FM polarons. The bulk of Monte Carlo snapshots (not shown), as taken from simulations for the FM Kondo model, contains isolated FM polarons of size $L_f = 3$ or $L_f = 4$. Once in a while two of them collide and form passing bi-polarons. The observed fraction of bi-polarons corresponds to a random distribution of polarons. In order to quantify the information revealed by the MC-snapshots, we introduce a modified corespin correlation function

$$S_n(l) = \frac{1}{L-l} \sum_{i=1}^{L-l} n_i^h \, \mathbf{S}_i \cdot \mathbf{S}_{i+l} \qquad (8)$$

that measures the corespin correlations in the vicinity of a charge carrier (hole). The density operator n_i^h for holes at site i is related to the density operator for electrons via $n_i^h = 1 - n_i$. Figure 4 shows the results of an unbiased grand canonical MC simulation. The observables are evaluated at different subspaces with a fixed particle number. We observe ferromagnetic correlations that vanish at $l = 3$ corresponding to a polaron that extends over $L_f = 4$ lattice sites. It should be pointed out that the MC result is almost independent of the number of holes in the system. In particular, the data do not indicate any enlargement of the FM domain for a larger number of holes. This result can only be explained by individual FM polarons because the size of the FM domain would
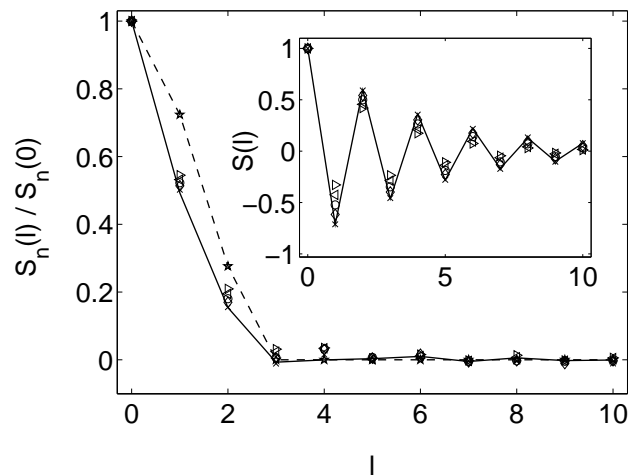

FIG. 4: Modified spin-spin correlation function from unbiased MC for an $L = 50$-site chain containing one ($\times$), two ($\diamond$), three ($\circ$), four ($\triangleleft$), and five ($\triangleright$) holes. The inset shows the conventional spin-spin correlation function $S(l) = \frac{1}{L-l} \sum_{i=1}^{L-l} \mathbf{S}_i \cdot \mathbf{S}_{i+l}$. The dashed line is calculated within the simple polaron picture, while the solid line represents the generalized UHA result for a single polaron. Parameters are $\beta = 50$, $J' = 0.02$, and $J_H = 6$.

strongly increase if there were two or more holes trapped in it.

The inset of Fig. 4 shows the conventional corespin correlation function $S(l)$. We observe the expected antiferromagnetic correlations, which decrease slightly with increasing number of holes.

The result for the modified spin-spin correlation function can again be explained qualitatively by the simple polaron picture. We consider a single polaron in which one charge-carrier is confined. Let the probability for the hole to be at site ν in the FM region be p_ν, which is roughly given by the result for a particle in an infinite potential well (see Fig. 1): $p_\nu \propto \sin^2(\nu \, \pi/(L_f + 1))$. The spin correlation is computed assuming perfect FM order inside the polaron and perfect AFM order outside. The result of this simple idea for $L_f = 4$ is shown as the dashed line in Fig. 4. It agrees qualitatively with the MC data.

For a quantitative, but still fairly simple description, we will now generalize the uniform hopping approximation, to allow for FM polarons.

IV. UHA FOR FM POLARONS

In the previous section we have interpreted the MC data by using the simplest polaron ideas. In what follows we will refine our polaron picture by including thermodynamic fluctuations of the corespins. This is done by a generalization of the finite-temperature uniform hopping approach (UHA) introduced in Ref 28.

In the spirit of UHA, the impact of the corespins on

the motion of the e_g electrons is now described by two UHA parameters, u_f and u_a, for the FM and AFM region, respectively. These two parameters are averages of the hopping amplitudes in the FM and AFM domains, respectively. Their distribution is given by a two-parameter density of states denoted by $\Gamma_{N_f,N_a}(u_f, u_a)$.

The size of individual polarons is fixed to L_f lattice sites. It is, however, possible that polarons overlap. The positions of the polarons are specified by the locations $\{i_1, \ldots, i_m\}$ of their left ends, where m is the number of FM polaron wells. If polarons overlap, they may form a bi-polaron or even greater accumulations of holes. The grand canonical partition function in this generalized UHA reads

$$\mathcal{Z} = \sum_m \sum_{\{i_1,\ldots,i_m\}} \iint_0^1 du_f du_a \, \Gamma_{N_f,N_a}(u_f, u_a) \, \operatorname{tr}_c e^{-\beta(\hat{H}(u_f,u_a;i_1,\ldots,i_m)-\mu\hat{N})} \; . \tag{9}$$

For 1D chains, subject to open boundary condition, the joint density $\Gamma_{N_f,N_a}(u_f, u_a)$ depends merely upon the number N_f (N_a) of bonds in FM (AFM) regions. In higher dimensions, $\Gamma_{N_f,N_a}(u_f, u_a)$ would actually depend upon the location of the individual polarons. The generalized UHA Hamiltonian reads

$$\hat{H}(u_f,u_a;i_1,\ldots,i_m) = -\sum_{<ij>} u_{ij} \, c_i^\dagger c_j - \frac{z}{2J_H} \sum_i \left(1 - \frac{1}{z}\sum_\delta u_{i,i+\delta}^2\right) n_i + J' \sum_{\langle ij \rangle}(2\, u_{ij}^2 - 1) \; , \tag{10}$$

where δ stands for n.n. vectors and z denotes the coordination number. The UHA parameter u_{ij} are either u_f or u_a, depending upon the type of magnetic order at the adjacent sites i and j. The integrand of the partition function in Eq. (9) defines the joint thermal probability density $p(u_f, u_a \,|\, \beta)$. From $p(u_f, u_a \,|\, \beta)$, we estimate mean values $\overline{u}_f, \overline{u}_a$ of u_f and u_a of a $L = 20$-site chain reading

$$\overline{u}_f = 0.937 \; , \quad \overline{u}_a = 0.31 \tag{11}$$

for the standard parameter set $J' = 0.02$ and $J_H = 6$ and $\beta = 50$. These mean values are independent of the number of polarons and their positions as long as the total volume of the polarons is small compared to the system size. In order to simplify the following discussion, we will replace the thermal averaging of an observable by the value of that observable at $\overline{u}_f, \overline{u}_a$. For the partition function this yields the simple form

$$\mathcal{Z} = \sum_m \sum_{\{i_1,\ldots,i_m\}} \operatorname{tr}_c e^{-\beta(\hat{H}(\overline{u}_f,\overline{u}_a;i_1,\ldots,i_m)-\mu(L-m))} \; , \tag{12}$$

where the influence of the thermal fluctuations of the corespins is contained in the average hopping amplitudes $\overline{u}_f$ and $\overline{u}_a$.

These average hopping amplitudes, however, are not sufficient for the determination of observables that do not directly derive from the partition function such as spin-spin correlations and one-particle spectral functions. In principle, these observables can be calculated in UHA by averaging over a set of *typical* thermal corespin configurations $\{\mathcal{S}\}$ obtained in UHA. In order to construct such a set, the azimuthal angles are also required, although they do not enter the energy and have a flat thermal probability density. The simplest way of constructing typical corespin configurations is to draw azimuthal angles at random. Starting from the reference spin $\mathbf{S}_\nu$ we proceed to the neighboring corespins by adding a random azimuthal angle χ to the fixed relative polar angle. Thus we obtain a collection of typical corespin configurations $\{\mathcal{S}\}$.

A. Static Correlations

We continue the discussion of the modified spin-spin correlation function $S_n(l)$. For a quantitative, but still fairly simple description, we take the deviations from perfect FM and AFM order into account, while for the hole the approximate probabilities p_ν are retained. We employ the mean UHA parameters $\overline{u}_f$ and $\overline{u}_a$ to describe the relative angles of neighboring corespins and average over typical corespin configurations with random hole positions. A comparison of the unbiased MC results with those of this approximate polaron approach, depicted in Fig. 4, reveals an excellent agreement.

Another observable to distinguish between polarons, bi-polarons, or even phase separated high density FM

clusters is the density-density correlation function

$$C(l) := \frac{1}{L-l} \sum_{i=1}^{L-l} \langle (n_i^h - \langle n_i^h \rangle)(n_{i+l}^h - \langle n_{i+l}^h \rangle) \rangle . \quad (13)$$

If holes form independent FM polarons, the correlation function should be structureless, while if holes gather in one FM regime, the correlation function will exhibit a positive peak at a typical inter-particle distance. In Fig. 5 $C(l)$ is shown for the two-hole subspace, where only those spin configurations of the Markov chain are taken into account, for which $N_h \simeq 2$. The UHA-polaron result is derived as follows. The positions of two FM-regions of size $L_f = 4$ are chosen at random, including overlapping ones. The hopping parameters are $\bar{u}_f$ ($\bar{u}_a$) for FM (AFM) bonds and the resulting tight-binding model is solved. The lowest two eigenstates will then be localized in the two FM potential wells. The resulting correlation functions are averaged over all possible positions of the FM potential wells. We observe a strikingly close agreement with the unbiased MC results. Similarly we proceed in the bi-polaron case, which is characterized by a single FM region of optimized size ($L_f = 7$). Here the two holes occupy the ground state and first excited state of the FM potential well. The resulting correlation function differs drastically from the MC data.
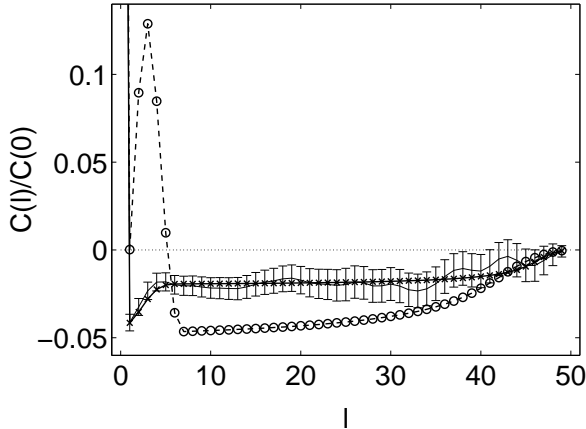

FIG. 5: Density density correlation function for $L = 50, \beta = 50, J' = 0.01, J_H = 6$, and $N_h = 2$. Error bars represent unbiased MC data, crosses stand for polaron-, and circles for bi-polaron results in UHA.

This discrepancy increases with increasing hole number, which shows clearly that the physics of the 1D FM Kondo model is correctly described by single-hole polarons and not by phase separation.

B. Polaronic features in the spectral density

In this subsection, we compute the spin-integrated spectral density

$$A_k(\omega) = -\frac{1}{\pi} \sum_\sigma \Im \ll a_{k\sigma}; a_{k\sigma}^\dagger \gg_\omega$$

for the original DE model by unbiased MC simulations based on the expression Eq. (6). The results will again be analyzed by UHA in the framework of the polaron ansatz. In particular the pseudogap in the spectral density near $n = 1$, found in the FM Kondo model[18,30], can readily be explained in the polaron picture. It is a consequence of the ferromagnetic box in which the hole moves.

The computation of $A_k(\omega)$ in UHA is based on the reasoning that led to the partition function in Eq. (12). I.e., for each polaron configuration and each value of $\bar{u}_a$, eigenvalues $\epsilon^{(\lambda)}$ and eigenvectors $|\psi^{(\lambda)}\rangle$ of the respective tight-binding Hamiltonian are determined, from which the Green's function

$$\ll c_i; c_j^\dagger \gg_\omega^{\bar{u}_a, \bar{u}_f} .$$

is determined in local spin-quantization. The transformation to the global spin-quantization is given by Eq. (6)

$$\sum_\sigma \ll a_{i\sigma}; a_{j\sigma}^\dagger \gg_\omega^{\mathcal{S}} = u_{j,i}^{\uparrow\uparrow}(\mathcal{S}) \ll c_i; c_j^\dagger \gg_\omega^{\bar{u}_a, \bar{u}_f} . \quad (14)$$

In the framework of UHA the relative angles of neighboring spins are fixed by the parameters $\bar{u}_a$ and $\bar{u}_f$. For a unique description of the entire spin configuration, however, azimuthal angles are again required. We proceed like in the discussion corresponding to Eq. (13), i.e. for fixed parameters $(\bar{u}_f, \bar{u}_a)$, spin configurations are generated with a flat sampling distribution in azimuthal angles. This is little numerical effort, as only the prefactor $u_{ij}^{\uparrow\uparrow}(\mathcal{S})$ is affected.

In the transition region ($\mu \simeq \mu^*$), the number of polaron wells is not well defined, as pointed out in conjunction with Fig. 3. In order to obtain a detailed understanding we compare unbiased MC data and results of the polaron ansatz in the subspace of fixed particle (polaron) number.

1. Antiferromagnetism at half filling

We begin the discussion with the spectrum of the AFM state for the completely filled lower Kondo band (no polarons). The unbiased MC data as shown in Fig. 6 display broad structures due to incoherent motion of charge carriers in a spin background that exhibits random deviations from perfect AFM order. The result can be described by the UHA ansatz. For the mean value of the hopping amplitude we have $\bar{u}_a = 0.31$ which corresponds to $\langle S_i S_{i+1} \rangle = \cos(\vartheta) \simeq -0.7$. Since there are no holes,
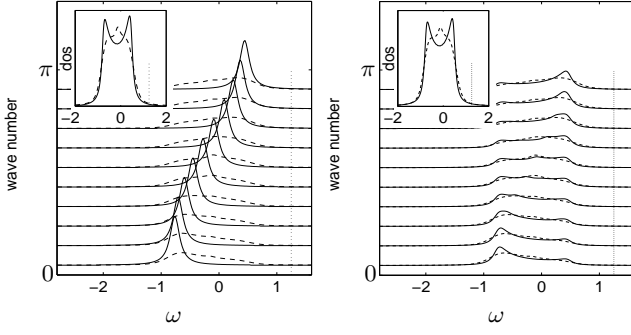
FIG. 6: Spectral density of a half-filled Kondo chain with parameters $L = 20, \beta = 50, J' = 0.02, J_H = 6$, and $\mu = 1.25$. Dashed lines represent unbiased MC data, solid lines stand for UHA result ($\bar{u}_a = 0.31$). Inset: density of states. The vertical bar indicates the chemical potential. The left(right)-hand panel shows UHA-results in local (global) spin quantization. Error bars have been omitted for clarity.

and consequently no polarons, the UHA parameters are the same for all bonds. The left-hand panel in Fig. 6 shows the UHA result in local quantization, i.e. without the transformation given in Eq. (14). In local quantization, the spectral density is simply given by

$$A_k(\omega) = \delta(\omega - 2\bar{u}_a \cos(k)) .$$

The agreement with the unbiased MC result is rather poor at this stage although the band width is already well approximated. In the MC spectra, only very weak remnants of the tight-binding features are visible on top of the incoherent spectrum, which is almost k-independent.

However, if we take into account the necessary transformation Eq. (14) to a global spin quantization, the agreement is strikingly close (see right-hand panel). The quasi-particle dispersion is strongly smeared out due to the random azimuthal angles of the corespins. There are two minor discrepancies between UHA and unbiased MC. The tight-binding remnants are more pronounced in UHA, while the MC results exhibit a weak structure near $\omega = 0$, which is due to random fluctuations in the relative n.n. angles, resulting in locally trapped electrons. Nonetheless, at half-filling UHA and unbiased MC simulations yield compatible results for the spectral density and the density of states (insets of Fig. 6).

2. Ferromagnetic Polarons

Next we consider the case of one hole in the otherwise half-filled Kondo chain. To this end, we investigate the grand canonical MC data in the $N_h = 1$ subspace. The respective MC spectrum is shown in Figs. 7 and 8. The main feature of the spectrum is a broad incoherent background, similar to the one found in the AFM case. In addition, two dispersionless structures are visible at $\omega \approx \pm 1.5$. As discussed earlier[18,30], a pseudogap shows up at the chemical potential. We find that an additional
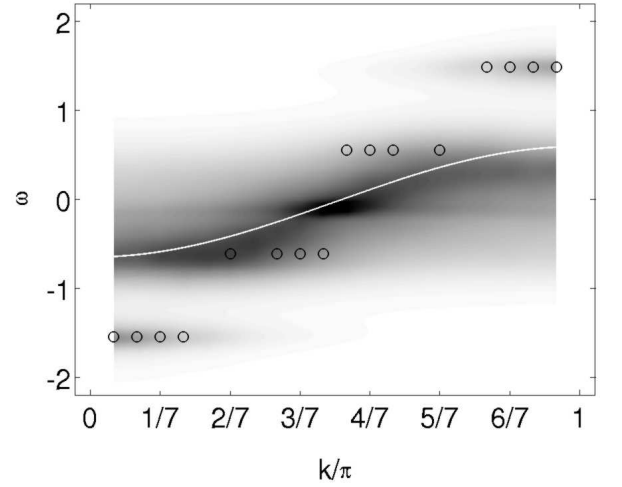

FIG. 7: Spectral density for $N_h = 1$ holes (one polaron). Parameters like in Fig. 6, except $\mu = 1.1$. Comparison of MC data (gray scale plot) with results of the simple polaron-well model. Circles (solid bright lines) stem from states localized in the FM (AFM)-well. Hopping parameters for the polaron-well model are $\bar{u}_f = 0.937$, $\bar{u}_a = 0.31$, and $L_f = 4$.

(mirror) gap appears at the opposite side of the spectrum.

Before discussing the UHA result, we want to provide a rough explanation of the MC data in terms of a simple polaron model. We assume an FM polaron-well of size $L_f = 4$, characterized by a tight-binding hopping parameter $\bar{u}_f$ embedded in an antiferromagnetic background with hopping parameter $\bar{u}_a$. Since the two hopping parameters are very different, we treat the various regions as separate chains and neglect their interaction. I.e. there is an isolated tight-binding chain of size L_f corresponding to the FM region, and one or two chains corresponding to the AFM background. A carrier is localized either in the FM or the AFM domain. The eigenvalues in the FM region, $\varepsilon_\nu^f = -2\bar{u}_f \cos(k_\nu^f)$, depend on the momentum $k_\nu^f = \nu\pi/(L_f + 1)$ with $\nu = 1, \ldots, L_f$. The energies of states corresponding to different localizations of the FM well ($i_0 = 1, \ldots, L - L_f$) are degenerate. The corresponding eigenstates in real space read

$$\psi_i^{(k_\nu, i_0)} \propto \begin{cases} \sin((i - i_0 + 1)k_\nu), & i_0 \leq i < i_0 + L_f \\ 0, & \text{otherwise.} \end{cases}$$

In this simple polaron-well model the expression for that part of the spectral density in local spin-quantization is

$$A_k^f(\omega) \propto \sum_{\nu=1}^{L_f} \sum_{i_0=1}^{L-L_f} \left| \langle k | \psi^{(k_\nu, i_0)} \rangle \right|^2 \delta(\omega - \epsilon_\nu^f)$$

$$\propto \sum_{\nu=1}^{L_f} c_\nu(k) \, \delta(\omega - \epsilon_\nu^f) , \qquad (15)$$

where $|k\rangle$ stands for the eigenvectors of the homogeneous tight-binding model with open boundary condition, i.e.
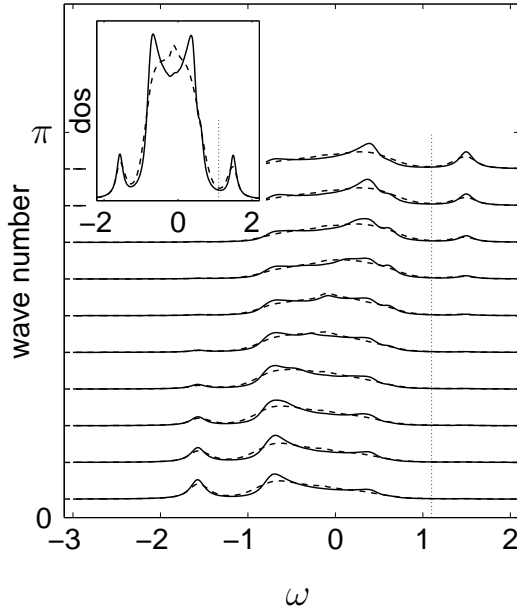
FIG. 8: Spectral density for $N_h = 1$ hole (one polaron). Symbols like in Fig. 6 and parameters like in Fig. 7. The broad incoherent central part of the spectrum (width $\simeq 2\bar{u}_a$) derives from the motion of the electrons in the fluctuating AFM background. Polaronic peaks show up at $\omega \simeq \pm 1.5$. In between these two structures a pseudogap opens at the chemical potential μ^*. It is accompanied by a mirror pseudogap near $-\mu^*$.

$\langle j|k\rangle \propto \sin(j\,k)$. The coefficient $c_\nu(k)$ as function of k shows a broad hump at $k \simeq k_\nu$. Hence, the contributions of the FM regions to $A_k(\omega)$ are dispersionless structures at energies $\omega = \epsilon_\nu^f$ which are concentrated about $k = k_\nu^f$. These structures are marked by open circles in the grayscale plot of Fig. 7. They explain the additional features at the band edges, which are clearly visible in the spectral density in addition to the broad incoherent background. The latter is due to the motion of the hole in the AFM regions. Since the AFM regions are much larger than the FM well, a continuous tight-binding band develops, characterized by the hopping parameter $\bar{u}_a$. The band is shown as a white line in Fig. 7. This part of the spectrum is similar to that at half filling (Fig. 6). The remaining discrepancy as compared to the MC data is due to the fluctuations of the azimuthal angles of the corespins causing the white line to become more incoherent, as shown by the UHA calculations below. The transformation from local to global spin-quantization has, however, negligible impact on the polaron states in the spectrum, since they are due to the FM region, in which the fluctuations of the corespins are less relevant. As we can see in Fig. 7, our reasoning based on a single polaron well already describes the qualitative features correctly.

The origin of the pseudogap and its 'mirror image' on the opposite side of the spectrum can now be simply identified as the energy difference between the upper most (lowest) state in the FM potential well ($E = \mp 2\bar{u}_f \cos(\pi/(L_f+1))$) and the upper (lower) edge of the tight-binding band in the AFM region ($E = \mp 2\bar{u}_a$) leading to a width of the pseudogap $\Delta E = 2(\bar{u}_f \cos(\pi/(L_f+1)) - \bar{u}_a)$, see Fig. 7.

A different picture would emerge if the FM domains were more extended, as for example in a PS scenario. They would then contain many energy levels (not only four as in Fig. 7) and should thus *not* give rise to a pseudogap.

For a more quantitative description we invoke the two-parameter UHA as described before. In Fig. 8 the UHA results, already in global quantization, are compared with those of unbiased MC simulations. The features of the spectral density are well reproduced. UHA even yields quantitative agreement as far as the pseudogap in the density of state is concerned.
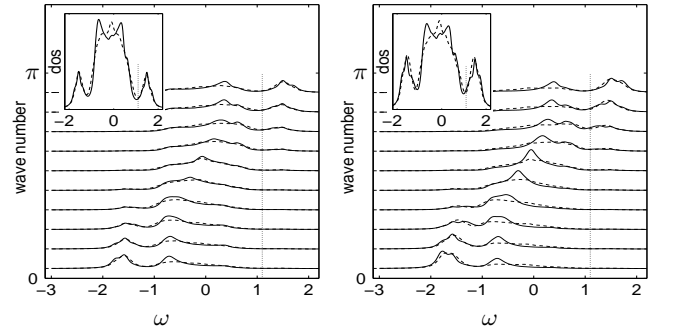

FIG. 9: Spectral density for $N_h = 2$ holes (two polarons) in the left-hand panel and $N_h = 3$ holes (three polarons) in the right-hand panel. Parameters and meaning of symbols like in Fig. 8.

For the same value of the chemical potential $\mu = 1.1$, the two- and three- hole subspaces have been studied by projecting the grand canonical MC data on the $N_h = 2$ and $N_h = 3$ subspace, respectively. The results are depicted in Fig. 9. The spectra are qualitatively similar to those for the one-hole subspace. Only the spectral weight of the polaron peak increases and shoulders show up in the AFM part of the spectrum. They are due to the interstitial AFM regions enclosed by the FM-polaron wells. The argument is the same as before. The allowed energies are $\varepsilon(k) = -2\bar{u}_a \cos(k)$, but now the possible k-values depend on the size of the interstitial regions.

C. Discussion

The emerging global picture is as follows. There exists a critical chemical potential μ^*. The value of μ^* can be obtained from simplified energy considerations. For μ significantly above μ^*, the band is completely filled and antiferromagnetic. The spectral density in this case is shown in Fig. 6. At μ^*, according to Fig. 3, holes enter the e_g-band forming isolated FM domains each containing a *single* hole (see Figs. 4 and 5). In the grand canoni-

cal ensemble, the number of polarons strongly fluctuates and the height of the polaron peak in the spectrum is directly linked to the number of holes. The pseudogap appears around the critical chemical potential. For values below μ^*, the system switches from predominantly AFM order to FM behavior and the pseudogap gradually disappears in favor of a single quasi particle band of tight-binding type. Our analysis yields compelling evidence against the PS scenario and in favor of FM polarons in 1D. Furthermore, it appears plausible that the formation of FM polarons will exist in symbiosis with lattice deformations (Jahn-Teller polarons)[6,25].

For CMR oxides, Saitoh et al [27] have investigated the temperature dependence of angle resolved photoemission spectra (ARPES) for the phase transition from FM to PM order. These studies show that a pseudogap also develops above T_C, which can be rationalized in the polaron picture. In the PM phase we have the competition of ferromagnetism, driven by the DE mechanism, and spin disorder due to thermal fluctuations. Therefore, FM polarons will form in the paramagnetic background. They will, however, be more extended because the PM force is less pronounced than the AFM force at low temperatures[3]. With increasing temperature, the corespin fluctuations become stronger and the competition of the FM polarons with the PM background gets tougher. The existence of FM domains above T_C has been corroborated by neutron scattering experiments[32].

Furthermore, the ARPES experiments revealed that the bandwidth changes merely by about 4% across the FM to PM phase transition. On the other hand, it has been argued[27] that the DE model predicts a reduction of about 30% in the PM phase if there the mean angle between neighboring spins is taken to be $\pi/4$ and the mean hopping parameter is therefore reduced to $1/\sqrt{2}$. The authors in Ref. 27 therefore conclude that 'DE is probably not even the dominant mechanism ...'.

At first glance, the argument seems convincing. However, in the polaron picture we do not really expect such a dramatic change of the band width since it is determined by the polaronic peaks at $E = \pm 2\bar{u}_f \cos(\pi/(L_f + 1))$. Hence, the band edges depend on the hopping parameter of the FM region and not on that of the PM region. Moreover, by the same reasoning that leads to a bandwidth reduction of 30% in the PM state, one would expect that the bandwidth vanishes in the AFM phase at low temperatures, since here the neighboring corespins are mostly antiparallel. That conclusion is in strong contrast to the unbiased MC results depicted in Figs. 8 and 9. Even for the incoherent inner part of the spectrum, which is due to electronic motion in the AFM region, a considerable band width exists, due to the spin fluctuations which are present even at very low temperatures. On top of that, the band-edges at finite hole filling are not really

determined by the AFM regime, but rather by the FM polarons.

V. CONCLUSIONS

In this paper, polaronic aspects of the ferromagnetic Kondo (double-exchange) model have been analyzed by unbiased finite temperature Monte-Carlo simulations and they have been explained by simple physical pictures. It has been found that in 1D, the physical effects of the FM Kondo model close to half filling are not governed by phase separation, as previously reported, but rather by single-hole ferromagnetic polarons. They can be explained qualitatively on the back of an envelope by idealized polaron pictures.

It seems sensible to reassess the explanations of CMR based on PS. These explanations are primarily based on percolation ideas, which can equally well be applied to FM polarons as percolating units. It appears plausible that the formation of FM polarons will exist in symbiosis with lattice deformations (Jahn-Teller polarons). Single-hole FM polarons allow a direct explanation of the pseudogap, observed in the manganites, whereas for larger FM clusters the pseudogap would be filled up by additional states. The striking similarity of the bandwidth of the FM and the PM phase, observed in ARPES experiments, can also be explained by FM polarons in the frame of the DE model. Moreover, the infinite compressibility near the half filled band, which has previously been attributed to PS, is a consequence of the fluctuating number of polarons in the grand canonical ensemble. Work is in progress for higher-dimensional systems where the entropy is expected to have less influence on the thermodynamic behavior.

For the analysis of the Monte Carlo results, we have extended the uniform hopping approach (UHA) at finite temperatures to include polaronic effects. This ansatz reduces the numerical effort by several orders of magnitude, while retaining all crucial physical features. The key idea is to map the physics of the high-dimensional configuration space of the t_{2g} corespins onto an effective two-parametric model. A full thermodynamic evaluation of the UHA model takes into account entropy and fluctuations of the corespins. The results are in close agreement with the unbiased MC data and allow a realistic description of all FM polaron effects found in various physical quantities.

VI.   ACKNOWLEDGEMENT

---

[*] Electronic address: koller@itp.tu-graz.ac.at

[1] T. Kaplan and S. Mahanti, *Physics of Manganites* (Kluwer

Academic/ Plenum Publishers, New York, Boston, Dordrecht, London, Moscow, 1998), 1st ed.

[2] E. L. Nagaev, *Colossal Magentoresistance and Phase Separation in Magnetic Semiconductors* (Imperial College Press, London, 2002), 1st ed.

[3] P. Horsch, J. Jaklic, and F. Mack, Phys. Rev. B **59**, R14149 (1999).

[4] J. Bala, A. M. Oles, and P. Horsch, Phys. Rev. B **65**, 134420/1 (2002).

[5] C. Zener, Phys. Rev. **82**, 403 (1951).

[6] D. M. Edwards, Adv. Phys. **51**, 1259 (2002).

[7] D. Meyer, C. Santos, and W. Nolting, J. Phys. Condens. Matter **13**, 2531 (2001).

[8] W. Müller and W. Nolting, Phys. Rev. B **66**, 085205 (2002).

[9] E. Dagotto, S. Yunoki, A. L. Malvezzi, A. Moreo, J. Hu, S. Capponi, D. Poilblanc, and N. Furukawa, Phys. Rev. B **58**, 6414 (1998).

[10] S. Yunoki and A. Moreo, Phys. Rev. B **58**, 6403 (1998).

[11] S. Yunoki, J. Hu, A. L. Malvezzi, A. Moreo, N. Furukawa, and E. Dagotto, Phys. Rev. Lett. **80**, 845 (1998).

[12] H. Yi, N. H. Hur, and J. Yu, Phys. Rev. B **61**, 9501 (2000).

[13] N. Furukawa, *in: Physics of manganites* (Kluwer Academic Publisher, New York, 1998), 1st ed.

[14] Y. Motome and N. Furukawa, J. Phys. Soc. Jpn. **69**, 3785 (2000).

[15] A. Chattopadhyay, A. J. Millis, and S. Das Sarma, Phys. Rev. B **64**, 012416 (2001).

[16] J. L. Alonso, L. A. Fernández, F. Guinea, V. Laliena, and V. Martín-Mayor, Nucl. Phys. B **569**, 587 (2001).

[17] J. L. Alonso, J. A. Capitán, L. A. Fernández, F. Guinea, and V. Martín-Mayor, Phys. Rev. B **64**, 54408 (2001).

[18] W. Koller, A. Prüll, H. G. Evertz, and W. von der Linden, Phys. Rev. B **66**, 144425 (2002).

[19] A. O. Sboychakov, A. L. Rakhmanov, K. I. Kugel, M. Y. Kagan, and I. V. Brodsky, J. Exp. Theor. Phys. **95**, 753 (2002).

[20] A. Moreo, S. Yunoki, and E. Dagotto, Science **283**, 2034 (1999).

[21] E. Dagotto, T. Hotta, and A. Moreo, Phys. Rep. **344**, 1 (2001).

[22] T. Wu, S. B. Ogale, J. E. Garrison, B. Nagaraj, A. Biswas, Z. Chen, R. L. Greene, R. Ramesh, T. Venkatesan, and A. J. Millis, Phys. Rev. Lett. **86**, 5998 (2001).

[23] P. Allen and V. Perebeinos, Phys. Rev. B **60**, 10747 (1999).

[24] S. Yunoki, A. Moreo, and E. Dagotto, Phys. Rev. Lett. **81**, 5612 (1998).

[25] A. J. Millis, R. Mueller, and B. I. Shraiman, Phys. Rev. B **54**, 5389 (1996).

[26] D. S. Dessau, T. Saitoh, C. H. Park, Z. X. Shen, P. Villella, N. Hamada, Y. Moritomo, and Y. Tokura, Phys. Rev. Lett. **81**, 192 (1998).

[27] T. Saitoh, D. S. Dessau, Y. Moritomo, T. Kimura, Y. Tokura, and N. Hamada, Phys. Rev. B **62**, 1039 (2000).

[28] W. Koller, A. Prüll, H. G. Evertz, and W. von der Linden, cond-mat **0211672** (2002).

[29] P.-G. de Gennes, Phys. Rev. **118**, 141 (1960).

[30] A. Moreo, S. Yunoki, and E. Dagotto, Phys. Rev. Lett. **83**, 2773 (1999).

[31] Y.-R. Chen and P. B. Allen, Phys. Rv. B **64**, 064401 (2001).

[32] T. G. Perring, G. Aeppli, and Y. Tokura, Phys. Rev. Lett. **78**, 3197 (1997).